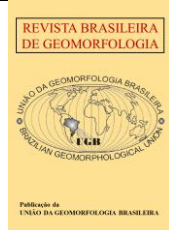




<https://rbgeomorfologia.org.br/>  
ISSN 2236-5664



## Research Article

# Determination and characterization of the junction angles in river channels in Brazil with Google Earth Pro images

## *Determinação e caracterização do ângulo de junção em canais fluviais no Brasil a partir de imagens do Google Earth Pro*

Marco Alésio Figueiredo Pereira <sup>1</sup>, Amanda de Souza Alves <sup>2</sup> e Masato Kobiyama <sup>3</sup>

<sup>1</sup> Universidade Feevale, Programa de Pós-graduação em Qualidade Ambiental, Novo Hamburgo, Brasil. E-mail. marco@feevale.br

ORCID: <https://orcid.org/0000-0001-5567-1491>

<sup>2</sup> Universidade Feevale, Programa de Pós-graduação em Qualidade Ambiental, Novo Hamburgo, Brasil. E-mail. amanda.alves.aa115@gmail.com

ORCID: <https://orcid.org/0000-0002-9079-606X>

<sup>3</sup> Universidade Federal do Rio Grande do Sul, Instituto de Pesquisas Hidráulicas, Porto Alegre, Brasil. E-mail. masato.kobiyama@ufrgs.br

ORCID: <https://orcid.org/0000-0003-0615-9867>

Received: 25/07/2023; Accepted: 18/06/2024; Published: 09/07/2024

**Abstract:** The determination of the junction angles and the river dynamics that form them have been studied since the 1930s. These studies normally have three approaches: reduced models, field investigation, and numerical simulation. To collaborate the scientific advances in this topic, the present study proposes a new methodology to determine junction angles in river channels, based on the Cosine Law, employing high-resolution remote sensing imagery. To verify your performance, 135 confluences located in six Brazilian biomes have been analyzed. These confluences were characterized with different magnitudes of channel width and different angles. Thus, relationship between width of the channels and their junction angles were evaluated, it has been obtained values  $\alpha$  between  $79^\circ$  and  $101^\circ$ , values  $\beta$  between  $133^\circ$  and  $150^\circ$  and values  $\gamma$  between  $117^\circ$  and  $140^\circ$ . Results show that the channel width influences the magnitude of the junction angles.

**Keywords:** Aerial images; Cosine Law; River confluence.

**Resumo:** A determinação dos ângulos de junção e as dinâmicas que ocorrem para formar esses ângulos tem sido objeto de estudo desde a década de 1930. O entendimento destes, pode ser dividido em modelos reduzidos, investigação em campo e simulação numérica. Assim, com o intuito de corroborar com o avanço científico nesta área do saber este estudo apresenta uma metodologia para a determinação dos ângulos de junção em canais fluviais, a partir da Lei dos Cossenos, utilizando imagens de sensoriamento remoto de alta resolução espacial. Para verificar seu desempenho foram analisadas 135 confluências distribuídas nos seis biomas brasileiros. Essas confluências foram caracterizadas com diferentes magnitudes de largura de canal e diferentes ângulos. Assim, foram avaliadas as relações entre a largura dos canais e seus ângulos de junção, obtendo-se valores  $\alpha$  entre  $79^\circ$  e  $101^\circ$ , valores  $\beta$  entre  $133^\circ$  e  $150^\circ$  e valores  $\gamma$  entre  $117^\circ$  e  $140^\circ$ . Os resultados mostram que a largura do canal influencia a magnitude dos ângulos de junção.

**Palavras-chave:** Imagens aéreas; Lei dos Cossenos; Confluência em rios.

## 1. Introduction

The junctions or confluences of channels are places in the drainage network where complex interactions between matter (water and sediment) and energy (stream power) occur, provided of the combination of two different flows (BEST, 1987; 1988; ROY, 2008; SANTOS; STEVAUX, 2017). The flow structure at this location depends mainly on three factors: junction angles, symmetry of the confluence plane, and the movement ratio (MOSLEY, 1976; BEST, 1987). In addition, these places are considered crucial points for the diversity of the ichthyofauna (YUAN et al., 2022). Due to fluctuations in flow structure, sediment transport, changes in channel morphology, and such complex interactions at the channel junction, these have been important objects for researchers in hydrology and hydraulics (CONSTANTINESCU, 2014; SUKHODOLOV et al., 2017; SUKHODOLOV; SUKHODOLOVA, 2019; GHOSH, 2019), hydrogeomorphology (VAN DENDEREN et al., 2018; JUNG; SHIN; PARK, 2019; SIQUEIRA; FILIZOLA, 2021) and ecology (BENDA et al., 2004; RICE et al., 2008).

The understanding of the junction angle establishment in river channels has been corroborated by several studies across various approaches. Santos and Stevaux (2017) identified three main categories: (i) laboratory experiments, using reduced models (ZHANG et al., 2015; YUAN et al., 2016; NAZARI-GIGLOU et al., 2016; LUDENÁ et al., 2017a,b; ALOMARI et al., 2018; LUO et al., 2018; PENNA et al., 2018; CANELAS et al., 2019; RAMOS et al., 2019; SZEWCZYK; GRIMAUD; COJAN, 2020); (ii) field surveys (ZINGER et al., 2013; PARK; LATRUBESSE 2015; RILEY et al., 2015; MORAIS et al., 2016; HOOSHYAR; SINGH; WANG, 2017; HACKNEY et al., 2018; GHOSH 2019; PEREIRA et al., 2019; LUZ et al., 2020; MARINHO et al., 2022); and (iii) numerical simulations (BRADBROOK; LANE; RICHARDS, 2000; BRADBROOK et al., 2001; BIRON; LANE 2008; QING-YUAN et al., 2009; CONSTANTINESCU et al., 2011; GEBEMARIAM 2017; PORNPROMMIN; IZUMI; PARKER, 2017; ZHOU et al., 2021).

Despite a number of studies on confluence in river channels, the main interest of the aforementioned studies has been directed towards understanding the flow behavior and interactions that occur within the channel. Some studies addressed how to measure the junction angle (HOOSHYAR; SINGH; WANG, 2017; BISWAS; PAL; PANI, 2019; YUKAWA; WATANABE; HARA, 2019; MENG et al., 2020); on the other hand, only one angle formed by two channels entering the confluence was investigated without mentioning the other two angles at the junction.

Pereira et al. (2019) compared junction angles values across three methods: imagery from Google Earth Pro, images collected with UAV (Unmanned Aerial Vehicle), and the minimum energy principle (ROY, 1983; WOLDENBERG; HORSFIELD, 1983). Therefore, the authors used only one confluence point, located in the Sinos River basin, southern Brazil.

Therefore, the main goal of this study was to validate the methodology presented by Pereira et al. (2019) using only satellite images to determine three types of junction angles in river channels, applying the Cosine Law. To verify your performance, confluences of river channels found throughout Brazil were analyzed, encompassing six different biomes. Then, the relationship between channel width and its junction angles was evaluated by biome.

## 2. Theoretical background

Studies related to junction angles are based on the assumptions presented by Mosley (1976) and improved by Best (1987), where the general model of flows for the open channel confluence zones consists of six different zones: flow stagnation region, flow deflection, flow separation, maximum velocity, flow recovery and shear layers. (BIRON; BEST; ROY, 1996; SHAKIBAINIA; TABATABAI; ZARRATI, 2010; RILEY; RHOADS, 2012; ZHANG et al., 2015; NAZARI-GIGLOU et al., 2016; SANTOS; STEVAUX, 2017).

The mathematical representation of these angles has been discussed since the precepts launched by Horton (1932) where the channels angles have been governed by line slope energy of the main and tributary channel. Subsequently, Howard (1971) argued that the junction angle in channels can be examined with the work rate (energy) given by gravity and the flow both downstream and upstream of the junction. He suggested that this connection occurs at a location where there is a minimum power rating ( $\Omega$ ). Building upon this concept, De Serres et al. (1999) noted that the flow predominance can be determined as a movement function.

Zamir (1976), Roy (1983), and Woldenberg and Horsfield (1983) stated that the junction angle is independent of the channel length ( $L_i$ ) emphasizing that the junction angle is a function of the minimum energy and that it can be expressed by the Cosine Law (Eq.1):

$$\cos \alpha = \frac{(S_0)^2 + (S_1)^2 - (S_2)^2}{2.S_1.S_2} \tag{1}$$

where  $S_0$ ,  $S_1$  and  $S_2$  are the channel gradients (energy slope) upstream and downstream of the main river and of the tributary, respectively.

**3. Data and methods**

*3.1. Determination of the junction point (p)*

It had been adopted the angles ( $\alpha$ ,  $\beta$  and  $\gamma$ ) of consolidated representation in the literature (HORTON, 1945; HOWARD, 1971; ROY, 1983; WOLDENBERG; HORSFIELD, 1983) (Figure 1). Thus, the junction angle  $\alpha$  is formed with two inlet channels,  $\beta$  is defined solely by the main river between upstream and downstream, and  $\gamma$  is formed by the tributary river and the main downstream. Determination of the central point ( $p$ ), from which the alignments will begin to infer the angles  $\alpha$ ,  $\beta$ , and  $\gamma$ , is an essential step to achieve accurate results of the junction angles. There is no standard method for this determination. Although Woldenberg and Horsfield (1983) addressed the issue of determining  $p$  using an analytical solution.

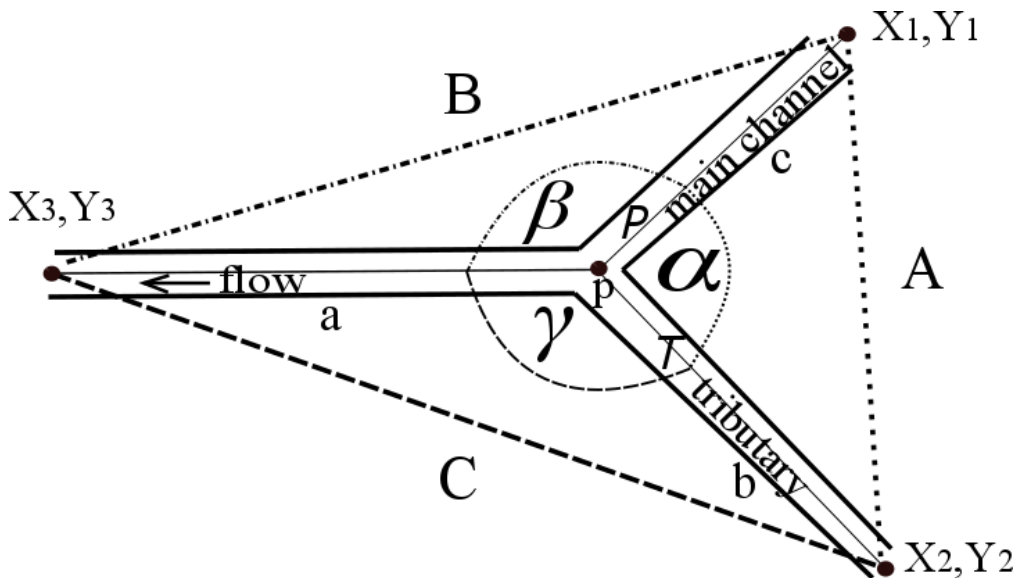


**Figure 1.** Representation of junction angles.

In the present study, the determination of point  $p$  consists of generating a circle that touches all the boundaries (margins) of the three channels (Figure 2a). The center point is defined as the intersection between two lines drawn vertically and horizontally in the middle of the circle. From this point, measure the distance of three channel widths, tangent to the circle (Figure 2b); this distance is suitable to account for channel adjustments in the immediate vicinity of the confluences (KLEINHANS et al., 2008; HACKNEY; CARLING, 2011). These alignments are extended to the middle of the river, where their widths are measured (Figure 2c), and points 1, 2, and 3 are defined (Figure 2d). From these segments, the values of  $\alpha$ ,  $\beta$ , and  $\gamma$  can be determined (Figure 2d).

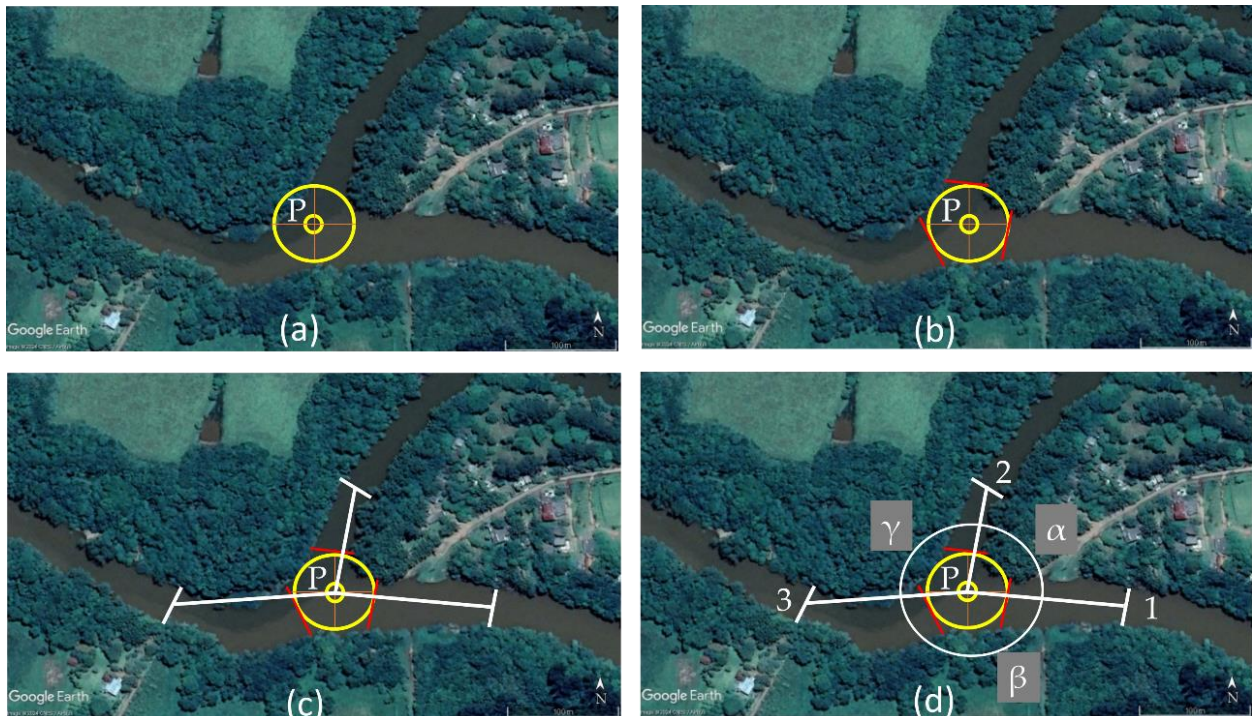


**Figure 2.** Representative scheme for junction angles determination: (a) application of the circumference to determine  $p$ ; (b) the channels width is the circle tangents (red lines); (c) extending the alignment to the middle of the channel; and (d) determination of  $\alpha$ ,  $\beta$  and  $\gamma$ . Note that the numbers 1 and 3 indicate the main channel upstream and downstream, respectively. The number 2 indicates the tributary channel.

In addition to determining  $\beta$  and  $\gamma$ , angles not covered by Hooshyar, Singh and Wang (2017), Seybold, Rothman and Kircner (2017), and Biswas, Pal and Pani (2019), the application of the proposed methodology can stand out in terms of ease and convention. In this case, it stands out because it does not require a mathematical basis or field surveys of channel flow, velocity, and slope.

### 3.2. Determination of the junction angle

Considering all the assumptions presented by (ZAMIR, 1976; ROY, 1983; WOLDENBERG; HORSFIELD, 1983; HOOSHYAR; SINGH; WANG, 2017; BISWAS; PAL; PANI, 2019; YUKAWA; WATANABE; HARA, 2019) the methodology of Pereira et al. (2019) was validated using aerial images from the Google Earth Pro website. For the determination of the respective angles, the Cosine Law applied (Eq. 2, 3, and 4):

$$\alpha = \cos^{-1} \frac{(b^2+c^2-A^2)}{(2 \cdot b \cdot c)} \tag{2}$$

$$\beta = \cos^{-1} \frac{(a^2+c^2-B^2)}{(2 \cdot a \cdot c)} \tag{3}$$

$$\gamma = \cos^{-1} \frac{(a^2+b^2-C^2)}{(2 \cdot a \cdot b)} \tag{4}$$

The determination of the horizontal distances of the  $a$ ,  $b$ ,  $c$ ,  $A$ ,  $B$ , and  $C$  alignments that make up the triangles for the application of the Cosine Law (Figure 1) can be done with the Euclidean distance (Eq. 5).

$$D = \sqrt{(X_{n+1} - X_n)^2 + (Y_{n+1} - Y_n)^2} \tag{5}$$

where  $D$  is the horizontal distance between the points of interest; and  $X_n$  and  $Y_n$  are the metric coordinate system of the respective points of interest.

Validation of values of  $\alpha$ ,  $\beta$  and  $\gamma$  have been verified through the normality test proposed by Shapiro and Wilk (1965), with a significance level of 5%. Furthermore, correlation analysis was performed between the analyzed angles and their respective channel widths using the Kendall method, with a p-value = 0.05 (see Table 1).

### 3.3. Junction Angle View

To represent the combination of  $\alpha$ ,  $\beta$  and  $\gamma$  values, it has been used the diagram proposed by Kobiyama et al. (2016). To trace the junction angles' point between these values, sloping and horizontal lines were drawn (Figure 3).

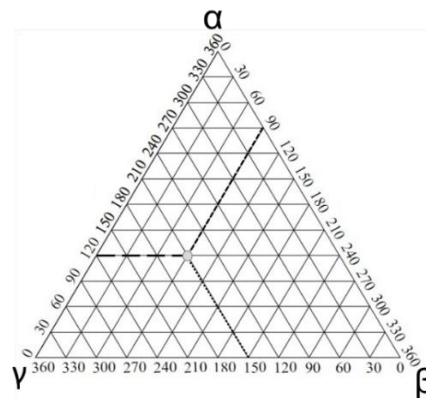


**Figure 3.** Diagram of representation of junction angles: Example for  $\alpha = 120^\circ$ ,  $\beta = 90^\circ$ , and  $\gamma = 150^\circ$ . Source: Adapted from Kobiyama et al. (2016).

### 3.4. Application

Using satellite images provided by Google Earth Pro, it has been selected 135 junction points (Figure 4), located in different Brazilian biomes. Due to the large territorial extension of the country ( $\approx 8 \cdot 10^6$  km<sup>2</sup>), the analyzed points are in distinct characteristics climatic, vegetation, hydrographic regions and soil types.

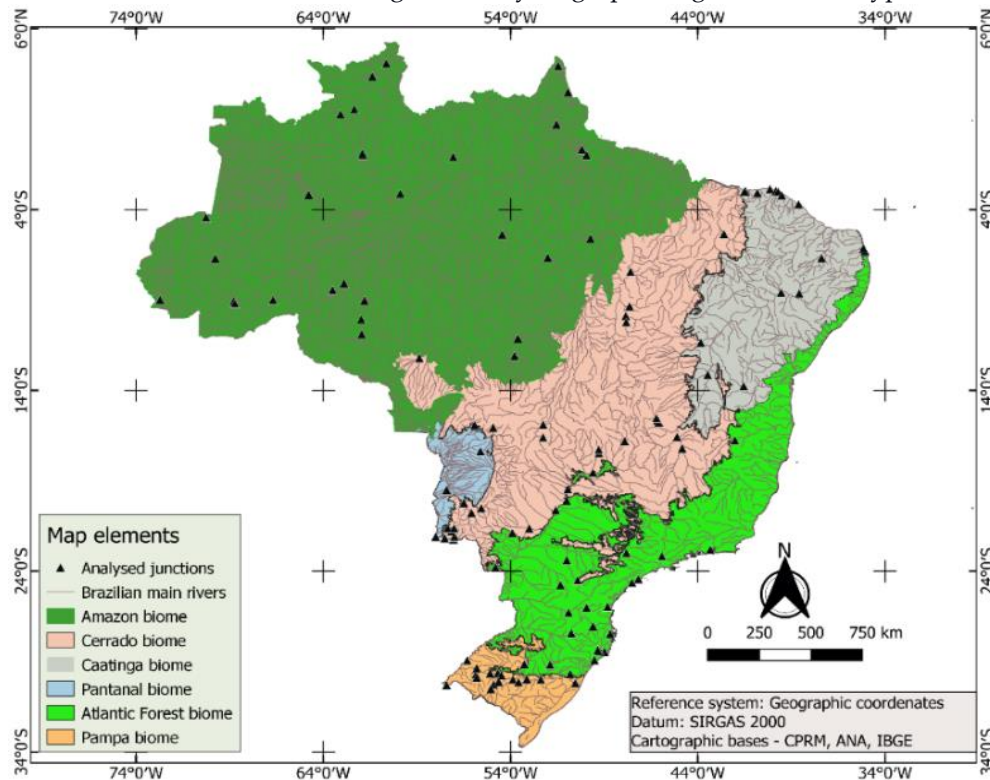


**Figure 4.** Location of confluence points analyzed different Brazilian biomes.

4. Results

Although the formation dynamics and changes in river channels are mainly governed by hydrogeomorphic processes, the purpose of measuring the junction angles to verify if there is a relationship between angles and channel width. Two examples of the proposed methodology are show in Figure 5. In this application we choose channels of different width and discharge. In the case of the Santa Maria (basin area = 10,451 km<sup>2</sup>) and Ibicuí rivers (State of Rio Grande do Sul) the channel widths in 1, 2 and 3 are 143 m, 126 m and 193 m respectively, near at the coordinate (Lat.= -30° 15' 16", Long.= -54° 53' 55"). In Figure 5b, the confluence of Solimões and Negro river in the Amazon River basin (basin area = 1,5x10<sup>6</sup> km<sup>2</sup>), where the widths in 1, 2 and 3 are 2,850 m, 1,900 m, and 2,500 m, respectively, near at the coordinate (Lat.= -03° 08' 06", Long.= -59° 54' 00"). In this case, we consider the area of the basin from the point of confluence for upstream.

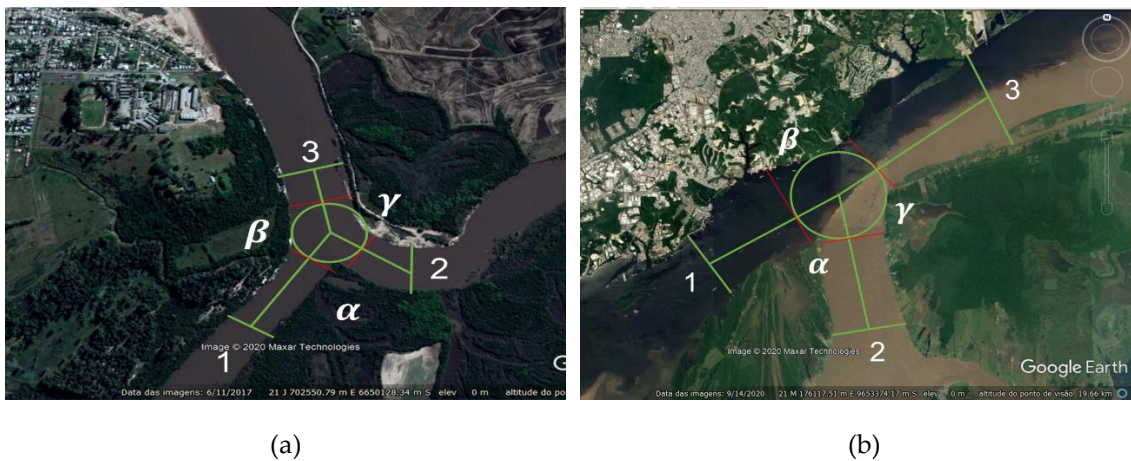


**Figure 5.** Representation of angles  $\alpha$ ,  $\beta$  and  $\gamma$ : (a) Santa Maria and Ibicuí river – Rio Grande do Sul State, Pampa biome; and (b) Rio Negro and Solimões rivers – Amazon State-Brazil, Amazon biome. The channel widths were measured with the green lines

Normality test proposed by Shapiro and Wilk (1965), with a significance level of 5%, was performed separately for each set of elements from each angle, as shown in Table 1. The results confirm that the samples come from a normal population. Additionally, the correlation test shows a strong correlation of the mean value of  $\beta$  with the width ( $P$ ) of the main channel upstream.

**Table 1.** Data basic statistical.

Angle	Normality test (Shapiro Wilk)		Correlation matrix (Kendall method)		
	Statistics	P-value	Angle	Channel width	
$\alpha$	0.983	0.722	Angle	1	0
			( $P$ )	0	1
$\beta$	0.964	0.843	Angle	1	0.8
			( $P$ )	0.8	1
$\gamma$	0.984	0.721	Angle	1	-0.4
			( $T$ )	-0.4	1

In Figure 6, the box plot illustrates the distribution of the junction angles, categorized by the Brazilian biomes.

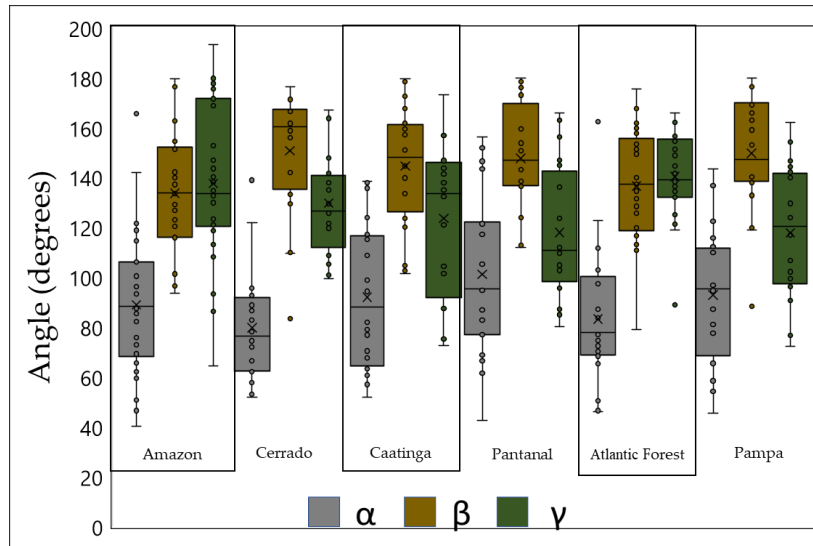


**Figure 6.** Junction angles in Brazilian biomes. Circles are the measured river channel angles  $x$  is the average angle, and the median is the horizontal line within the box.

Table 2 details the predominant mean angles observed within each biome. In relation to the  $\alpha$ , the predominant angles are between  $61^\circ$  to  $120^\circ$  for all biomes, as shown in the highlighted values. For the  $\beta$ , this predominance occurs between  $121^\circ$  to  $180^\circ$  for all biomes; and for the  $\gamma$ , this predominance also occurs between  $121^\circ$  to  $180^\circ$ , except the biome Pampa and biome Pantanal.

**Table 2.** Junction angle predominance.

Biome	Angle	Points by angle opening		
		$\alpha$	$\beta$	$\gamma$
Amazon	0-60	5	0	0
	61-120	21	9	7
	121 -180	4	21	23
Cerrado	0-60	4	0	0
	61-120	14	2	6
	121 -180	2	18	14
Caatinga	0-60	2	0	0
	61-120	15	4	7
	121 -180	3	16	13
Pantanal	0-60	1	0	0
	61-120	13	4	12
	121 -180	6	16	8
Atlantic Forest	0-60	3	0	0
	61-120	21	7	2
	121 -180	1	18	23
Pampa	0-60	4	0	0
	61-120	13	0	10
	121 -180	3	20	10

## 5. Discussion

The statistical normality of junction angles was previously studied by Hooshyar, Singh and Wang (2017). They utilized data from the Digital Elevation Model (DEM) provided by the USGS (United States Geological Survey), with a spatial resolution of 1 m. The study covered 120 basins located in 17 states of United States of America (USA), with drainage areas ranging from 0.04 to 3.5 km<sup>2</sup>. They observed the probability distribution function to follow a normal distribution. When analyzing approximately 20,000 confluences in Japan using digital maps at a scale of 1:25,000, Yukawa, Watanabe and Hara (2019) likewise observed that the distribution of angles approximately follows a Gaussian distribution.

Statistical inferences demonstrate the same tendency of normality for the analyzed data (Table 1). Therefore, it is assumed that the high correlation between channel width and angle  $\beta$ , as shown Table 1, is due to the width of the main channel. In other words, the greater the width of the main channel, the closer angle  $\beta$  will be to 180°, resulting in a more rectilinear channel. Additionally, it is also observed that angle  $\gamma$  exhibits a moderately negative correlation with the tributary channel width (T). This suggests that as the width of the tributary channel increases, there is a tendency for this channel to flow at a 90° angle into the main channel. Ranjbar et al. (2018) evaluated 26 basins in the USA with different climates and found that the length of the channel and its width are directly related, and that these variables influenced the pattern of the drainage network.

The mean value of  $\alpha$  is smaller than those of  $\beta$  and  $\gamma$  for all the Brazilian biomes (Figure 6), which is expected since  $\alpha$  represents the angle formed between the main upstream channel and the tributary (Figure 2D). The mean values of  $\beta$  are by 20°, 21°, 29°, and 31° larger than those of  $\gamma$  in the Cerrado, Caatinga, Pantanal and Pampa biomes, respectively. This difference is justified by  $\beta$  being the external angle formed between the main upstream and downstream channels (Figure 2D). However, in the Amazon and Atlantic Forest biomes, the mean value of  $\gamma$  is slightly higher than that of  $\beta$  by about 4°. This can be explained by the magnitude of the tributary channel, as discussed above.

The mean values of  $\alpha$  found to be 89°, 79°, 92°, 101°, 83°, and 92° for the Amazon Biome, the Cerrado Biome, the Caatinga Biome, the Pantanal Biome, the Atlantic Forest Biome, and the Pampa Biome, respectively. Hooshyar, Singh and Wang (2017) found  $\alpha$  values ranging from 45° for smaller contribution basin areas (0.04 Km<sup>2</sup>) and 75° for the larger ones (3.5 Km<sup>2</sup>). Seybold, Rothman and Kircner (2017), in study conducted in the USA, found  $\alpha$  values around of 45° in the driest regions and around 72° in the humid regions. Yukawa, Watanabe and Hara (2019), using data from literature, made statistical inferences found values around 72°. This research found larger values for  $\alpha$ , which can be explained, mainly by watersheds areas, there is an increase in  $\alpha$  values as the basin area increases (RANJBAR et al., 2018).

Most of  $\alpha$  values were between 61 to 120°,  $\beta$  values were mostly between 121° to 180°, while the  $\gamma$  values were between 61 to 120° in the Pantanal and Pampa biome, in other biomes values were between 121° to 180° (Table 2).

A relationship between the angles  $\alpha$ ,  $\beta$ , and  $\gamma$  with the channel width close to their respective confluences has been evaluated (see Table 3). In situations where  $P > T$ , the  $\beta$  values are larger than  $\alpha$  in all biomes, and the same relation can be also observed for  $\gamma$ , except in the Atlantic Forest biome. When  $T > P$ , there is an increase in the value of  $\alpha$  and a decrease in the value of  $\beta$  in the Amazon, Caatinga, and Pantanal biomes. In the Cerrado, Atlantic Forest, and Pampa biomes there is a decrease in  $\alpha$ , and an increase in  $\gamma$ . This result when  $T > P$  can be explained by the higher flow of tributary in relation to the main channel. There is a tendency for these angles to approach 90° the greater their flow energy in relation to the main channel.

It is observed that after the junction point, there is an increase in the width of the main channel downstream, with the greatest increase in the Caatinga biome, followed by the Atlantic Forest, Cerrado, Pampa, Amazon, and Pantanal biomes, with percentage values of 27%, 20%, 18%, 13%, 10%, and 4%, respectively.

The relationship between the width of the tributary channel and the width of the channel main upstream and downstream of the confluences was analyzed, in a study conducted in the Mekong River, Southeast Asia (Hackney, Carling, 2011). It was observed that, a slight narrowing occurred immediately below tributary junctions. However, with progression downstream, there is an increase in width. Furthermore, the observed relationship is shown to vary considerably with geology. The geological control suggests that complex factors play important roles in determining changes to channel width across large systems, and that simple cause–effect relationships do not hold.



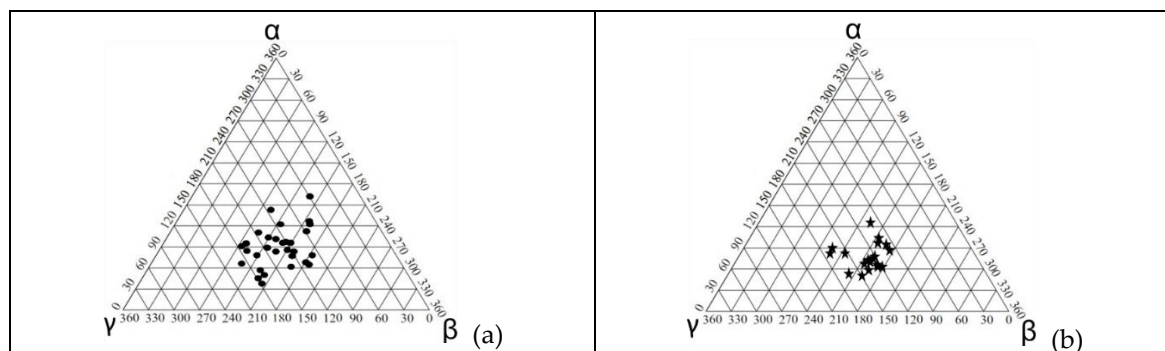
**Table 3.** Variation of junction angles  $\alpha$ ,  $\beta$ , and  $\gamma$ , with the channel widths situations.

Biome	Angle	$P > T$	$T > P$
Amazon	$\alpha$	88 ↓	101 ↑
	$\beta$	134 ↑	128 ↓
	$\gamma$	138 ↑	131 ↓
Cerrado	$\alpha$	80 ↑	77 ↓
	$\beta$	151 ↑	146 ↓
	$\gamma$	129 ↓	137 ↑
Caatinga	$\alpha$	90 ↓	124 ↑
	$\beta$	147 ↑	101 ↓
	$\gamma$	123 ↓	135 ↑
Pantanal	$\alpha$	87 ↓	118 ↑
	$\beta$	153 ↑	130 ↓
	$\gamma$	120 ↑	112 ↓
Atlantic Forest	$\alpha$	86 ↑	68 ↓
	$\beta$	134 ↓	150 ↑
	$\gamma$	140 ↓	142 ↑
Pampa	$\alpha$	93 ↑	91 ↓
	$\beta$	151 ↑	146 ↓
	$\gamma$	116 ↓	123 ↑

Note that  $P$  is the width of the main upstream channel,  $T$  is the width of the tributary channel, ↑ means an increase in the angle value and ↓ means a decrease in the angle value.

In the dispersion values of the 135 points (Figure 7), it can be observed that the mean values of  $\alpha$ ,  $\beta$ , and  $\gamma$  for each biome are similar. This suggests that there is no conjunction dynamics of the channels due to the biome in terms of junction angles. In relation to the  $\alpha$ , for all biomes, mean angle it is  $89^\circ$ , with most value for Pantanal biome with  $95^\circ$ , and lower value for Cerrado biome with  $80^\circ$ . For the  $\beta$ , mean angle it is  $144^\circ$ , with most value for Cerrado biome with  $151^\circ$ , and lower value for Amazon biome with  $134^\circ$ . For the  $\gamma$ , mean angle it is  $128^\circ$ , with most value for Atlantic Forest biome with  $140^\circ$ , and lower value for Pantanal biome and Pampa biome with  $118^\circ$  (Figure 7g).

We do not discuss the hydraulic and hydrogeomorphological factors acting on the formation and changes in fluvial channels, as the rivers analyzed have different magnitudes. Santos and Stevaux (2017) point out that large rivers drain areas that are significantly different in geological and climatic terms. Parsons et al. (2008) emphasize that the relationship of the main hydraulic variables defined for medium rivers, such as slope channel versus bankfull discharge (Leopold; Wolman, 1957) and slope versus width/depth ratio (Parker, 1976), does not apply to mega rivers with a flow greater than  $17,000 \text{ m}^3 \text{ s}^{-1}$  (LATRUBESSE, 2008).



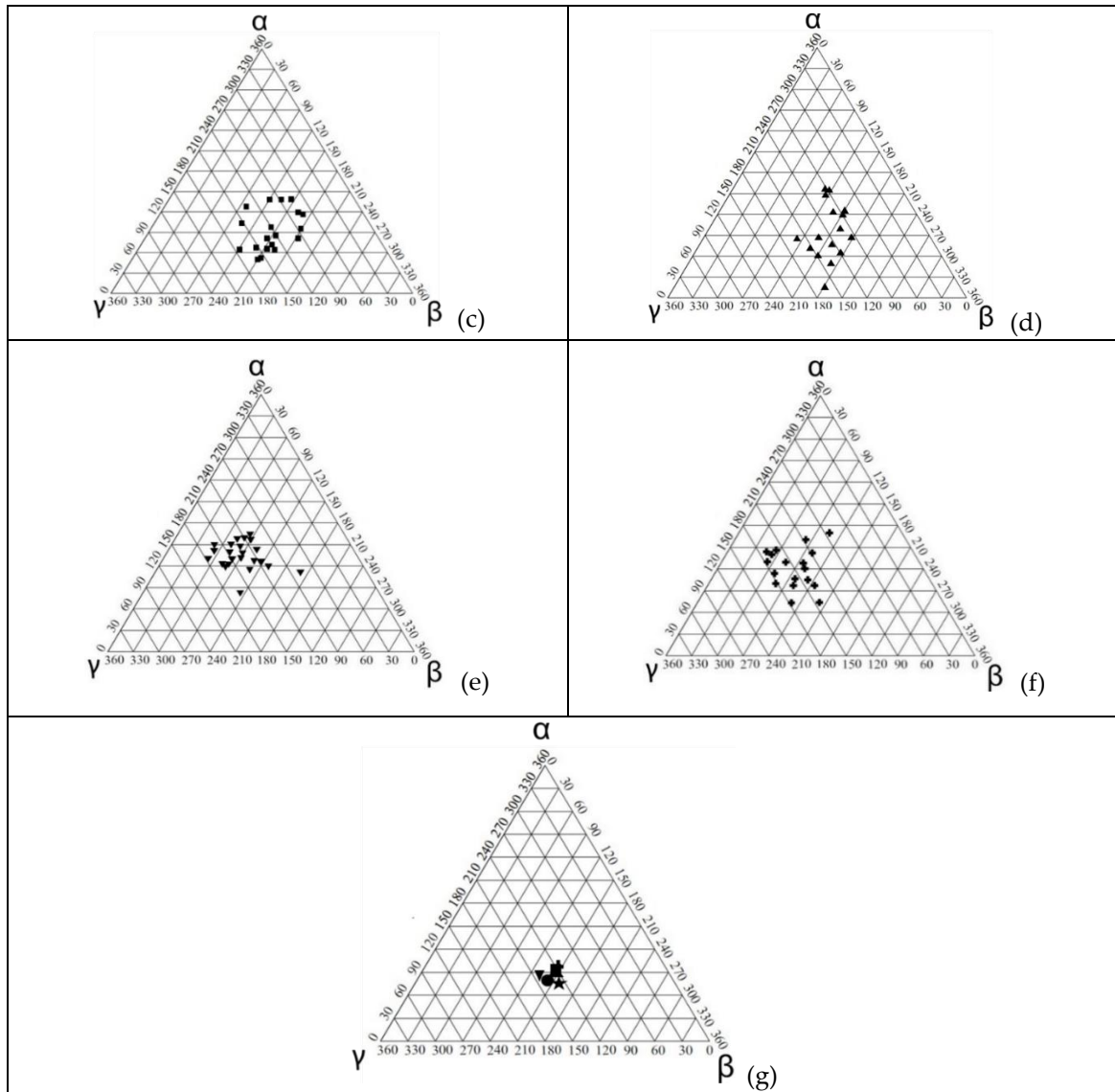


**Figure 7.** Junction angles diagram in the six Brazilian biomes: (a) Amazon; (b) Cerrado; (c) Caatinga; (d) Pantanal; (e) Atlantic Forest; (f) Pampa; and (g) Average angles for each biome.

### 5.1. Methodology limitations

The proposed methodology has a few limitations to be considered. For example, the image to be analyzed must have a spatial resolution (pixel) smaller than the channel width. Generally, the images provided by Google Earth Pro come from the satellites World View 1, 2, and 3 ( $\pm 30$  cm), Quickbird (60 cm), Ikonos (1 m), Spot (1.5 m) and Landsat (15-30 m) among other satellites and aerial images from other sources. Thus, the spatial resolution of the study site must be verified.

Another limitation is associated to the confluence type. In case of rivers with perennial confluences, but during the drought period, it is not possible to define the channel width and consequently the coordinates of the points 1, 2 and 3. In case of rivers with very dense riparian vegetation which covers both sides of the riverbank, it is not possible to correctly define the channel width.

In addition, some geomorphic settings can cause the difficulty to apply this methodology, such as confluence under the influence of a reservoir; rivers having a much smaller affluent flow than the mainstream; anamastomosing channel confluences; islands inside the river; and deltas. In this case, the determination of the point *p* cannot be executed correctly.

Although this methodology has some limitations, there are still advantages compared to other existing approaches. For example, it only applies Cosine Law on georeferenced images to determine the joint angles, which makes this methodology more robust and more mathematically accessible. In this context, it is not necessary to

measure parameters in the field, such as discharge or to perform topographic surveys to obtain bank and energy slope. Simply, from a computer with Internet access and freely available images, it is possible to determine the junction angles of river channels anywhere on the planet, considering the limitations aforementioned. With the historical availability of images over the same point, the methodology can be applied to assess the occurrence of changes over a long period.

## 6. Conclusions

This paper proposes a new methodology to determine junction angles in river channels based on the Cosine Law, by employing high-resolution remote sensing imagery. Through these images, it is not necessary to measure parameters in the field, such as discharge, or to perform topographic surveys, such as width and channel gradients (energy slope) to determine yours angles. Simply put, from a computer with Internet access and freely available images, it is possible to determine the joint angles of river channels anywhere on the planet, considering the previously mentioned limitations. Furthermore, with the historical availability of images over the same point, the methodology can be applied to assess the occurrence of changes over a long period.

Moreover, we analyzed the relationship between the angles  $\alpha$ ,  $\beta$ , and  $\gamma$  with the width of the main and tributary channels. Our findings demonstrate a direct relationship between main channel width and angle  $\beta$ ; in other words, the greater the width of the main channel, the closer angle  $\beta$  will be to  $180^\circ$ , resulting in a more rectilinear channel. Regarding angle  $\gamma$ , it is observed to have a moderately negative correlation with the tributary channel width. This suggests that as the width of the tributary channel increases, there is a tendency for this channel to flow at a  $90^\circ$  angle into the main channel.

As well, it is observed that after the junction point, there is an increase in the width of the main channel downstream.

Assessing junction angles using the Brazilian biomes as limiting factors. Our analysis indicates that mean value of  $\alpha$  is smaller than those of  $\beta$  and  $\gamma$  for all the Brazilian biomes. The mean values of  $\beta$  are larger than those of  $\gamma$  in the Cerrado, Caatinga, Pantanal and Pampa biomes, respectively. However, in the Amazon and Atlantic Forest biomes, the mean value of  $\gamma$  is slightly higher than that of  $\beta$  by about  $4^\circ$ .

In Brazilian biomes there is a great lithological heterogeneity, a preponderant factor in the formation of channels, so for future research, it is recommended to evaluate the angles as a function of the type of rock. Furthermore, another preponderant factor, not used in this research, is the inclusion of the channel order ( $\omega$ ), and contributing area of the channels.

**Author's contributions:** Conception, M.A.F.P. and M.K.; Methodology, M.A.F.P.; Validation, M.A.F.P. and A.S.A.; Research, A.S.A. and M.A.F.P.; Data preparation, A.S.A. and M.A.F.P.; Writing, M.A.F.P.; Revision, M.K. All authors read and agreed with the published version of the manuscript.

**Acknowledgments:** The second author thank to Feevale Scientific Initiation Program – PICF. All authors greatly thank the editor and two anonymous reviewers for their helpful and critical suggestions to improve the manuscript.

**Conflict of Interest:** The authors declare that there is no conflict of interest; the sponsors had no interference in the development of the study, in the collection, analysis, or interpretation of data, in the writing of the manuscript, or in the decision to publish the results.

## References

1. ALOMARI, N.K., YUSUF, B., MOHAMMAD, T.A., GHAZALI, A.H. Experimental investigation of scour at a channel junctions of different diversion angles and bed width ratios. *Catena*. v. 166, p. 10-20, 2018. DOI: 10.1016/j.catena.2018.03.013
2. BENDA, L., ANDRAS, K., MILLER, D., BIGELOW, P. Confluence effects in rivers: Interactions of basin scale, network geometry, and disturbance regimes. *Water Resources Research*, v. 40, n. 5, 2004. DOI: 10.1029/2003WR002583
3. BEST, J.L. Flow dynamics at river channel confluences: Implications for sediment transport and bed morphology. Recent Devel. In: ETHERIDGE, F. G.; FLORES, R. M.; HARVEY, M. D. *Fluvial Sedimentology*, Spec. Publ. 39. Tulsa Oklahoma, U.S.A.: Ed. SEPM (Society for Sedimentary Geology), 1987. p. 27-35. DOI: 10.2110/pec.87.39.0027
4. BEST, J.L. Sediment transport and bed morphology at river channel confluences. *Sedimentology*, v. 35, n. 3, p. 481-498, 1988. DOI: 10.1111/j.1365-3091.1988.tb00999.x

5. BIRON, P., BEST, J.L., ROY, A.G. Effects of bed discordance on flow dynamics at open channel confluences. **Journal Hydraulic Engineering**, v. 122, n. 12, p. 676-682, 1996. DOI: 10.1061/(ASCE)0733-9429(1996)122:12(676)
6. BIRON, P.M., LANE, S.N. Modelling hydraulics and sediment transport at river confluences. In: RICE, S.P.; ROY, A.G.; RHOADS, B.L. **River confluences, tributaries and the fluvial network**, England: Ed. John Wiley & Sons Ltd, 2008, p. 17-43. DOI: 10.1002/9780470760383.ch3
7. BISWAS, S.S., PAL, R., PANI P. Application of remote sensing and GIS in understanding channel confluence morphology of Barakar river in western most fringe of lower Ganga Basin. In: DAS, B.C., GHOSH, S., ISLAM, A. **Quaternary geomorphology in India: Case Studies from the Lower Ganga Basin**. Springer International Publishing, 2019. p. 139-153. DOI: 10.1007/978-3-319-90427-6\_8
8. BRADBROOK, K.F., LANE, S.N., RICHARDS, K.S. Numerical simulation of three-dimensional time-averaged flow structure at river channel confluences. **Water Resources Research**, v. 36, n. 9, p. 2731-2746, 2000. DOI: 10.1029/2000WR900011
9. BRADBROOK, K.F., LANE, S.N., RICHARDS, K.S., BIRON, P.M., ROY, A.G. Role of bed discordance at asymmetrical river confluences. **Journal of Hydraulic Engineering**, v. 127, n.5, p. 351-368, 2001. DOI: 10.1061/(ASCE)0733-9429(2001)127:5(351)
10. CANELAS, O.B., FERREIRA, R.M.L., LUDEÑA, S.G., ALEGRIA, F.C., CARDOSO, A.H., Three-dimensional flow structure at fixed 70° open-channel confluence with bed discordance. **Journal of Hydraulic Research**. v. 58, n. 3, p. 434-446, 2019. DOI: 10.1080/00221686.2019.1596988
11. CONSTANTINESCU, G., MIYAWAKI, S., RHOADS, B., SUKHODOLOV, A., KIRKIL, G. Structure of turbulent flow at a river confluence with momentum and velocity ratios close to 1: insight provided by an eddy-resolving numerical simulation. **Water Resources Research**. v. 47, n.5, 2011. DOI: 10.1029/2010WR010018
12. CONSTANTINESCU, G. LE of shallow mixing interfaces: A review. **Environmental Fluid Mechanics**, v. 14, n. 5, p. 971-996, 2014. DOI: 10.1007/s10652-013-9303-6
13. DE SERRES B., ROY, A.G., BIRON, P.M., BEST, J.L. Three-dimensional structure of flow at a confluence of river channels with discordant beds. **Geomorphology**, v. 26, n. 4, p. 313-335, 1999. DOI: 10.1016/S0169-555X(98)00064-6
14. GEBEMARIAM, T.K. Numerical Analysis of Stormwater Flow Conditions and Separation Zone at Open-Channel Junctions. **Journal of Irrigation and Drainage Engineering**, v. 143, n. 1, 2017. DOI: 10.1061/(ASCE)IR.1943-4774.0001114
15. GHOSH, K.G. Flow dynamics at channel confluences: few observations from a sub-tropical plateau fringe river of Eastern India. **Arabian Journal of Geosciences**. v. 12, 2019. DOI: 10.1007/s12517-019-4576-9
16. HACKNEY, C.R., CARLING, P. The occurrence of obtuse junction angles and changes in channel width below tributaries along the Mekong River, south-east Asia. **Earth Surface Processes Landforms**. v. 36, p. 1563-1576, 2011. DOI: 10.1002/esp.2165
17. HACKNEY, C.R., DARBY, S.E., PARSONS, D.R., LEYLAND, J., AALTO, R., NICHOLAS, A.P., BEST, J.L. The influence of flow discharge variations on the morphodynamics of a diffuence-confluence unit on a large river. **Earth Surface Processes Landforms**. v. 43, n. 2, p. 349-362, 2018. DOI: 10.1002/esp.4204
18. HOOSHYAR, M., SINGH, A., WANG, D. Hydrologic controls on junction angle of river networks. **Water Resources Research**. v. 53, n. 5, p. 4073-4083, 2017. DOI: 10.1002/2016WR020267
19. HORTON, R.E. Drainage Basin Characteristics. **Transactions of the American Geophysical Union**. v. 13, p. 350 - 361, 1932. DOI: 10.1029/TR013i001p00350
20. HORTON, R.E. Erosional development of stream and their drainage basins, hydro physical approach to quantitative morphology. **Bulletin of the Geological Society of America**, v. 56, p. 275-370, 1945. DOI: 10.1130/0016-7606(1945)56[275:EDOSAT]2.0.CO;2
21. HOWARD, A.D. Optimal angles of stream junction: Geometric, stability to capture and minimum power criteria. **Water Resources Research**, v. 7, n. 4, p. 863-873, 1971. DOI: 10.1029/WR007i004p00863
22. JUNG, K., SHIN, J.Y., PARK, D. A new approach for river network classification based on the beta distribution of tributary junction angles. **Journal of Hydrology**, v. 572, p. 66-74, 2019. DOI: 10.1016/j.jhydrol.2019.02.041
23. KLEINHANS, M.G, JAGERS H.R.A., MOSSELMAN E., SLOFF C.J. Bifurcation dynamics and avulsion duration in meandering rivers by one-dimensional and three-dimensional models. **Water Resources Research**, v. 44, n. 8, 2008. DOI: 10.1029/2007WR005912
24. KOBAYAMA, M., GODOY, Z.J.V., PEREIRA, M.A.F, MICHEL, G.P., MELO, C.M. Análise do ângulo de junção com consideração da hierarquização fluvial de Strahler e Shreve. In: XI Simpósio Nacional De Geomorfologia – SINAGEO, **Anais...** Ed. União da Geomorfologia Brasileira - UGB-, 2016, Maringá – PR, 8p.
25. LATRUBESSE, E.M. Patterns of anabranching channels: The ultimate end member adjustment of mega rivers. **Geomorphology**, v. 101, n. 1-2, p. 130-145, 2008. DOI: org/10.1016/j.geomorph.2008.05.035

26. LEOPOLD, L.B., WOLMAN, M. G. River channel patterns - braided, meandering, and straight. **U. S. Geological Survey Professional Paper**, v. 282, p. 39-85, 1957. DOI: 10.3133/pp282B
27. LUDEÑA, S.G., FRANCA, M.J., ALEGRIA, F., SCHLEISS, A.J., CARDOSO, A.H. Hydromorphodynamic effects of the width ratio and local tributary widening on discordant confluences. **Geomorphology**, v. 293, p. 289–304, 2017a. DOI: 10.1016/j.geomorph.2017.06.006
28. LUDEÑA, S.G., CHENG, Z., CONSTANTINESCU, G., FRANCA, M.J. Hydrodynamics of mountain river confluences and its relationship to sediment transport, **Journal Geophysical Research: Earth Surface**, v. 122, n. 4, p. 901–924, 2017b. DOI: 10.1002/2016JF004122.
29. LUO, H., FYTANIDIS, D.K., SCHMIDT, A.R., GARCÍA, M.H. Comparative 1D and 3D numerical investigation of open-channel junction flows and energy losses. **Advances in Water Resources**, v. 117, p. 120–139, 2018. DOI: 10.1016/j.advwatres.2018.05.012
30. LUZ, L.D., SZUPIANY, R.N., PAROLIN, M., SILVA, A., STEVAUX, J.C. Obtuse-angle vs. confluent sharp meander bends: insights from the Paraguay-Cuiabá confluence in the tropical Pantanal wetlands, Brazil. **Geomorphology**, v. 348, 2020. DOI: 10.1016/j.geomorph.2019.106907
31. MARINHO, R.R., FURTADO, A.R., SANTOS, V.C.D, NASCIMENTO, A.Z.A., FILIZOLA, N.P.J. Riverbed morphology and hydrodynamics in the confluence of complex mega rivers - A study in the Branco and Negro rivers, Amazon basin. **Journal of South American Earth Sciences**, v.18, p. 103969, 2022. DOI: 10.1016/j.jsames.2022.103969
32. MENG, X., ZHANG, P., LI, J., MA, C., LIU, D., The linkage between box-counting and geomorphic fractal dimensions in the fractal structure of river networks: the junction angle. **Hydrology Research**, v. 51, n. 6, p. 1397–1408, 2020. DOI: 10.2166/nh.2020.082
33. MORAIS, E. S. de, SANTOS, M.L. dos, CREMON, E.H., STEVAUX, J.C., Floodplain evolution in a confluence zone: Paraná and Ivaí rivers, Brazil. **Geomorphology**, v. 257, n. 15, p. 1–9, 2016. DOI: 10.1016/j.geomorph.2015.12.017
34. MOSLEY, M. P. An experimental study of channel confluences. **Journal of Geology**, v. 84, n. 5, p. 535-562, 1976. DOI: 10.1086/628230
35. NAZARI-GIGLOU, A., JABBARI-SAHEBARI, A., SHAKIBAEINIA, A., BORGHEI, S. M., An experimental study of sediment transport in channel confluences. **International Journal of Sediment Research**, v. 31, n. 1, p. 87–96, 2016. DOI: 10.1016/j.ijsrc.2014.08.001
36. PARK, E., LATRUBESSE, E.M. Surface water types and sediment distribution patterns at the confluence of mega rivers: The Solimões-Amazon and Negro Rivers junction. **Water Resources Research**, v. 51, n. 8, p. 6197–6213, 2015. DOI: 10.1002/2014WR016757.
37. PARKER, G. On the cause and characteristic scales of meandering and braiding in rivers. **Journal of Fluid Mechanics**, v. 76, n. 3, p. 457-480, 1976. DOI: 10.1017/S00222112076000748
38. PARSONS, D. R., BEST, J.L., LANE, S.N., KOSTASCHUK, R.A., HARDY, R.J., ORFEO, O., AMSLER, M.L., SZUPIANY, R.N. Large River Channel Confluences. In: RICE, S.P.; ROY, A.G.; RHOADS, B.L. **River confluences, tributaries and the fluvial network**. England: Ed. John Wiley & Sons Ltd, 2008. p. 74-118. DOI: 10.1002/9780470760383.ch5
39. PENNA, N., DE MARCHIS, M.; CANELAS, O.B.; NAPOLI, E.; CARDOSO, A.H.; GAUDIO, R. Effect of the Junction Angle on Turbulent Flow at a Hydraulic Confluence. **Water**, v. 10, n. 4, 2018. DOI: 10.3390/w10040469
40. PEREIRA, M. A. F., BARBIEIRO, B.L., CARNEIRO, M., KOBİYAMA, M., Determination of the junction angle in fluvial channels from georeferenced aerial images from Google Earth Pro and UAV. **Ambiente & Água - An Interdisciplinary Journal of Applied Science**, v.14, n. 5, 2019. DOI: 10.4136/ambi-agua.2345
41. PORNPROMMIN, A., IZUMI, N., PARKER, G. Initiation of Channel Head Bifurcation by Overland Flow. **Journal of Geophysical Research: Earth Surface**, v. 122, p. 2348 – 2369, 2017. DOI: 10.1002/2016JF003972
42. QING-YUAN, Y., XIAN-YE, W., WEI-ZHEN, L., XIE-KANG, W. Experimental Study on Characteristics of Separation Zone in Confluence Zones in Rivers. **Journal of Hydrologic Engineering**, v. 14, n. 2, p. 166-171, 2009. DOI: 10.1061/(ASCE)1084-0699(2009)14:2(166)
43. RANJBAR, S., HOOSHYAR, M., SINGH, A., WANG, D. Quantifying climatic controls on river network branching structure across scales. **Water Resources Research**, v. 54, p. 7347–7360, 2018. DOI: 10.1029/2018WR022853
44. RAMOS, P. X., SCHINDFESSEL, L., PÊGO, J.P., MULDER, T. Influence of bed elevation discordance on flow patterns and head losses in an open-channel confluence. **Water Science and Engineering**, v. 12, n. 3, p. 235-243, 2019. DOI: 10.1016/j.wse.2019.09.005
45. 00, S.P., KIFFNEY, P., GREENE, C., PESS, G.R. The ecological importance of tributaries and confluences. In: RICE, S.P.; 0, A.G.; RHOADS, B.L. **River confluences, tributaries and the fluvial network**, England: Ed. John Wiley & Sons Ltd, 2008, 210-242. DOI: 10.1002/9780470760383.ch11

46. RILEY, J.D., RHOADS, B.L. Flow structure and channel morphology at a natural confluent meander bend. **Geomorphology**, v. 13, n. 3, p. 84–98, 2012. DOI: 10.1016/j.geomorph.2011.06.01
47. RILEY, J.D., RHOADS, B.L., PARSONS, D.R., JOHNSON, K.K., Influence of junction angle on three-dimensional flow structure and bed morphology at confluence meander bends during different hydrological conditions. **Earth Surface Processes and Landforms**, v. 40, n. 2, p. 252–271, 2015. DOI: 10.1002/esp.3624
48. ROY, A.G. Optimal Angular Geometry Models of River Branching. **Geographical Analysis**, v. 15, n. 2, p. 87–96, 1983. DOI: 10.1111/j.1538-4632.1983.tb00771.x
49. ROY, A.G. River Channel Confluences. In: RICE, S.P.; ROY, A.G.; RHOADS, B.L. **River confluences, tributaries and the fluvial network**. England: Ed. John Wiley & Sons Ltd, 2008. p. 13–16. DOI: 10.1002/9780470760383.ch2
50. SANTOS, V. C. DOS, STEVAUX, J.C. Processos fluviais e morfologia em confluências de canais: uma revisão. **Revista Brasileira de Geomorfologia**, v. 18, n. 1, 2017. DOI: 10.20502/rbg.v18i1.1042
51. SEYBOLD, H., ROTHMAN, D., KIRCNER, J.W. Climate's watermark in the geometry of stream networks. **Geophysical Research Letters**, v. 44, n. 5, p. 2272–2280, 2017. DOI: 10.1002/2016GL072089
52. SHAKIBAINIA, A., TABATABAI, M.R.M., ZARRATI, A.R. Three-dimensional numerical study of flow structure in channel confluences. **Canadian Journal of Civil Engineering**, v. 37, n. 5, p. 772–781, 2010. DOI: 10.1139/L10-016
53. SHAPIRO, S.S., WILK, M.B. An Analysis of Variance Test for Normality (Complete Samples). **Biometrika**, 52, p. 591–611, 1965.
54. SIQUEIRA, L. F., FILIZOLA, N.P.J. Estudo hidrológico do efeito de barramento hidráulico no rio Tarumã-Açu, Manaus-AM. **Revista Brasileira de Geomorfologia**, v. 22, n. 2, 2021. DOI: 10.20502/rbg.v22i2.1752
55. SUKHODOLOV, A.N., KRICK, J., SUKHODOLOVA, T.A., CHENG, Z., RHOADS, B.L., CONSTANTINESCU, G.S. Turbulent flow structure at a discordant river confluence: Asymmetric jet dynamics with implications for channel morphology. **Journal of Geophysical Research: Earth Surface**, v. 122, n. 6, p. 1278–1293, 2017. DOI:10.1002/2016JF004126
56. SUKHODOLOV, A.N., SUKHODOLOVA, T.A. Dynamics of Flow at Concordant Gravel Bed River Confluences: Effects of Junction Angle and Momentum Flux Ratio. **Journal of Geophysical Research: Earth Surface**, v. 124, n. 2, 2019. DOI: 10.1029/2018JF004648
57. SZEWCZYK, L., GRIMAUD, J.L., COJAN, I. Experimental evidence for bifurcation angles control on abandoned channel fill geometry. **Earth Surface Dynamics**, v. 8, n. 2, p. 275–288, 2020. DOI: 10.5194/esurf-8-275-2020
58. VAN DENDEREN, R.P., SCHIELEN, R.M.J., BLOM, A., HULSCHER, S.J.M.H., KLEINHANS, M.G. Morphodynamic assessment of side channel systems using a simple one-dimensional bifurcation model and a comparison with aerial images. **Earth Surf. Process. Landforms**, v. 43, n. 6, p. 1169–1182, 2018. DOI: 10.1002/esp.4267
59. WOLDENBERG, M.J., HORSFIELD, K. Finding the Optimal Lengths for Three Branches at a Junction. **Journal Theoretical Biology**, v. 104, n. 2, p. 301–318, 1983. DOI: 10.1016/0022-5193(83)90417-4
60. YUAN, S., TANG, H., XIAO, Y., QIU, X., ZHANG, H., YU, D. Turbulent flow structure at a 90-degree open channel confluence: Accounting for the distortion of the shear layer. **Journal of Hydro-environment Research**, v. 12, p. 130–147, 2016. DOI: 10.1016/j.jher.2016.05.006
61. YUAN, S., XU, L., TANG, H., XIAO, Y., GUALTIERI, C. The dynamics of river confluences and their effects on the ecology of aquatic environment: A review. **Journal of Hydrodynamics**, v. 34, p. 1–14, 2022. DOI: 10.1007/s42241-022-0001-z
62. YUKAWA, S., WATANABE, T., HARA, K. Bifurcation Angle Distribution in the Japanese River Network. **Journal of the Physical Society of Japan**, v. 88, n. 2, 2019. DOI: 10.7566/JPSJ.88.024901
63. ZAMIR, M. Optimal Principles in Arterial Branching. **Journal Theoretical Biology**, v. 62, p. 227–251, 1976.
64. ZHANG, Y. WANG, P., WU, B.; HOU, S. An experimental study of fluvial processes at asymmetrical river confluences with hyper concentrated tributary flows. **Geomorphology**, v. 230, p. 26–36, 2015. DOI: 10.1016/j.geomorph.2014.11.001
65. ZHOU, J. ZENG, C., ZHOU, Z., WANG, L., YIN, Y. Energy and momentum correction coefficients within contraction zone in open-channel combining flows. **Water Science and Engineering**, v. 14, n. 4, p. 337–344, 2021. DOI: 10.1016/j.wse.2021.09.002
66. ZINGER, J. A., RHOADS, B.L., BEST, J.L., JOHNSON, K.K. Flow structure and channel morphodynamics of meander bend chute cutoffs: A case study of the Wabash River, USA. **Journal of Geophysical Research: Earth Surface**, v. 118, n. 4, p. 2468–2487, 2013. DOI: 10.1002/jgrf.20155



This work is licensed under the Creative Commons License Attribution 4.0 Internacional (<http://creativecommons.org/licenses/by/4.0/>) – CC BY. This license allows for others to distribute, remix, adapt and create from your work, even for commercial purposes, as long as they give you due credit for the original creation.